Available online at www.sciencedirect.com
ScienceDirect
Ceramics International 37 (2011) 1601–1607
CERAMICS INTERNATIONAL
www.elsevier.com/locate/ceramint

A comparative physico-chemical study of bioactive glass and bone-derived hydroxyapatite

A. Doostmohammadi [a,b,*], A. Monshi [a], M.H. Fathi [a], O. Braissant [c]

[a] Biomaterials Group, Materials Engineering Department, Isfahan University of Technology, Isfahan 84156-83111, Iran
[b] Isfahan University of Medical Science, Isfahan 81746-73461, Iran
[c] Laboratory of Biomechanics & Biocalorimetry, Coalition for Clinical Morphology & Biomedical Engineering, University of Basel, Faculty of Medicine, Basel, Switzerland

Received 25 November 2010; received in revised form 30 November 2010; accepted 19 January 2011
Available online 9 March 2011

Abstract

This study aimed at comparing the physico-chemical properties of bioactive glass and bone-derived hydroxyapatite (HA). 63S bioglass particles were obtained by sol–gel process and HA samples were derived from bovine bone. The chemical composition and the crystalline structure of both bioceramics were evaluated. Then the zeta potential in physiological saline and at different pH values was determined. It was found that the negativity of zeta potential for 63S bioglass is higher than that of bone-derived HA. The exothermal behavior through the hydration process was evaluated by isothermal microcalorimetry. The results showed that the librated heat during bioactive glass hydration process and its rate are almost ten times higher than HA. It could be related to different hydration mechanisms of bioglass and HA. However, for both bioglass and HA, this value is in the safe range and cannot be harmful for the adjacent tissues in the body.

Keywords: C. Chemical properties; E. Biomedical applications; Bioglass; Hydroxyapatite

1. Introduction

In recent years, the application of bioceramics used as the implant materials, has faced an increasing growth [1,2]. One of the most important reasons for welcoming these kinds of materials is their excellent biocompatibility and in some cases their considerable bioactivity in comparison with metallic and polymeric biomaterials [1]. Due to their special and distinctive features, bioactive glass and hydroxyapatite occupy a high place among different types of bioceramics [1–3]. Many researchers around the world are working on these materials; and their application in the human body is still expanding [1,2,4].

Bioactive glasses (SiO_2 glasses containing Ca and P) are popular materials for use in implant applications [1]. It is a non-resorbable biomaterial that has been favored since three decades ago for its reported advantages of forming a strong bond with living tissues, including bone and soft connective tissue [1,3]. Additionally, recent findings have demonstrated that there is a genetic control of the cellular response to bioactive glass materials [5]. Seven families of genes are up-regulated when primary human osteoblasts are exposed to the ionic dissolution products of bioactive glasses [5,6]. These findings indicate that bioactive glass materials are very engaging options for tissue regeneration and tissue engineering.

Hydroxyapatite (HA), $[Ca_{10}(PO4)_6(OH)_2]$, products are well-known as implantable ceramics for hard tissue reconstitution [7]. Hydroxyapatite is based on calcium phosphate, and its chemical composition and crystal structure are similar to the mineral component of human bones and teeth [8]. Consequently, it can be expected to be neither antigenic nor cytotoxic. This has proved to be so [9] and thus HA products are generally biocompatible. Hydroxyapatite supports osteoconduction [7–10], and after implantation and over time, HA materials derived from both natural and synthetic sources can gradually make a strong bounding to human bone tissue. Likewise, HA can be slowly replaced by the host bone tissue after implantation. Therefore HA is known as a suitable bone repair material [11].

* Corresponding author at: Biomaterials Group, Materials Engineering Department, Isfahan University of Technology, Isfahan 84156-83111, Iran. Tel.: +98 913 326 6632; fax: +98 311 3912751.
E-mail address: Alidm14@ma.iut.ac.ir (A. Doostmohammadi).

0272-8842/$36.00
doi:10.1016/j.ceramint.2011.03.009

In this study, first there would be a description of how the bioactive glass and bone-derived HA particles were prepared. Then, the physico-chemical properties of these two well-known bioceramics such as the zeta potential and heat of hydration were compared.

2. Materials and methods

2.1. Synthesis and preparation

2.1.1. Bioactive glass

Colloidal solutions (sols) of 63S composition (63 mol% SiO_2, 28 mol% CaO, 9 mol% P_2O_5) were prepared by mixing distilled water, 2 N hydrochloric acid, tetraethyl orthosilicate (TEOS), triethyl phosphate (TEP) and calcium nitrate [12]. The initial procedure involved mixing TEOS (28 ml) and ethanol (40 ml) as an alcoholic media. Distilled water was added to solution and allowed to mix until the solution became clear. The H_2O:(TEOS) molar ratio was 4:1. After 30 min, TEP (2.3 ml) was added to the stirring solution. After another 20 min, calcium nitrate (12 g) was added. The solution was then stirred for an additional hour. The gel was heated (60 °C, 10 h), dried (130 °C, 15 h) and thermally stabilized (600 °C, 2 h) according to established procedures [12,13]. The produced gel was ground with a mortar and pestle to disagglomerate the particles. Finally the particles were sieved to make a distribution of particles of size less than 5 μm (L3-M5 5 μm stainless steel sieve & Sonic Sifter Separator, Advantech Manufacturing Co., New Berlin, WI, USA). Bioactive glass particles were sterilized at 180 °C for 1 h.

2.1.2. Bone-derived HA

A femur of an adult bovine was obtained from a slaughter-house and boiled in water for 12 h to render it aseptic and loosen any attached soft tissues. Then it was washed and cleaned carefully to remove visible tissues, fats and any other readily visible foreign materials on the bone surface. To remove the internal organic content (e.g. collagen) and water, the bone was then heated in an electric furnace under ambient conditions, at 700 °C, with a 2 h holding time. The resulting white solid specimens were first ground and crushed with a mortar and pestle to produce a powder. The powder was then sieved to produce a distribution of particles of size less than 5 μm (L3-M5 5 μm stainless steel sieve & Sonic Sifter Separator, Advantech Manufacturing Co., New Berlin, WI, USA). Bone powders were sterilized at 150 °C for 1 h, rinsed in distilled water and incubated in 1% phosphoric acid. They were rinsed again in sterile distilled water, and sterilized at 200 °C.

2.2. Elemental composition analysis

The elemental composition of bioactive glass particles was confirmed by X-ray fluorescence spectroscopy (XRF), (PW2404, PHILIPS) and energy dispersive X-ray analysis (EDX) technique (SUPRA 40 VP FE-SEM).

Elemental analysis of the bone-derived HA particles was carried out using an energy dispersive X-ray fluorescence spectrometry (EDXRF) instrument (SPECTRO XEPOS, SPECTRO Analytical Instruments GmbH, Germany). A spectral resolution of less than 160 eV for Mn K-alpha was achieved and the maximum count rate was 120,000 cps.

2.3. Phase analysis by X-ray diffraction (XRD)

Phases present and gross chemical composition of the bioactive glass and HA particles were determined with an X-ray diffraction (XRD) instrument (X'Pert-MPD system with a Cu Kα wavelength of 1.5418 Å, Phillips, Netherlands). The diffractometer was operated at 40 kV and 30 mA at a 2θ range of 20–80° employing a step size of 0.02°/s.

2.4. Particle morphology by scanning electron microscopy (SEM)

Particle samples were mounted on aluminum SEM pins and coated with Au/Pd using a sputter coating instrument. They were then observed with a scanning electron microscope (SUPRA 40 VP FE-SEM, Carl Zeiss AG, Germany) operated at an acceleration voltage of 20 kV, and the images were stored as computer files.

2.5. Particle dispersion stability by zeta potential measurement

The zeta potential of the particles was measured with a laser Doppler electrophoresis (LDE) instrument (Nano Series, Malvern Instrument Ltd., United Kingdom). To roughly simulate in vivo ionic environments, bioactive glass and HA samples were suspended in physiological saline (0.154 M NaCl solution) at pH 3, 5, 7.4, 9 and 11. The suitability of such in vitro studies was addressed by Bagambisa et al. [14], who found that an aqueous in vitro model yielded complementary results when compared to the in vivo results because of the ubiquitous presence of water.

The potential was determined six times (each measurement being the average of 40 runs) and the mean values and standard deviations were calculated. The instrument automatically calculates electrophoretic mobility (U), and zeta potential according to Smoluchowski's equation [15]:

$$\zeta = \frac{U\eta}{\varepsilon} \quad (1)$$

where ζ is the zeta potential, U the electrophoretic mobility, η the medium viscosity and ε is the dielectric constant.

2.6. The exothermal behavior in the hydration process by isothermal microcalorimetry

When bioceramics are mixed with aqueous solutions, heat of hydration is liberated. The amount of hydration heat and the hydration rate of 63S bioactive glass and bone-derived HA particles were determined by isothermal microcalorimetry and compared with each other. The tests were carried out applying 5 different relative humidities and using the humidity chamber

Table 1
The amount of relative humidity in different prepared samples for evaluation of heat hydration.

Sample	Salt solution	Relative humidity (%)	Weight of bioceramic (mg)
1	Only water	100	50
2	KNO_3	91	50
3	KCl	84	50
4	NaCl	75	50
5	$MgCl_2$	32	50
6	Only water	100	0
7	KNO_3	91	0
8	KCl	84	0
9	NaCl	75	0
10	$MgCl_2$	32	0

methods. In this method, five different saturated salt solutions were prepared in HPLC inserts and enclosed in microcalorimetric ampoules, therefore, allowing a constant relative humidity in such a closed system [16]. 50 mg of each bioceramic particles, i.e. bioactive glass and HA, were placed in the microcalorimetric ampoules, and each cell was added with one HPLC insert filled with 200 μl of saturated salt solution. Also five control samples were prepared containing only the saturated salt solution in its insert. The prepared samples and the amount of relative humidity in different samples are shown in Table 1. The ampoules were sealed and introduced in a TAM48 microcalorimeter (TAM, Thermal Activity Monitor 48, Waters/TA Instrument, New Castle, DE).

3. Results

3.1. Elemental composition analysis

3.1.1. EDX and XRF results for bioactive glass

The result of EDX microanalysis of the glass particles is shown in Fig. 1. The peaks of O, Si, P and Ca indicated the consisting elements of prepared bioactive glass particles.

The existent elements in prepared bioactive glass particles and estimated composition measured by X-ray fluorescence (XRF), is shown in Table 2. The molar percentage of oxides was expressed by the computer according to the elemental analysis and with the assumption that all the elements were in oxidic form.

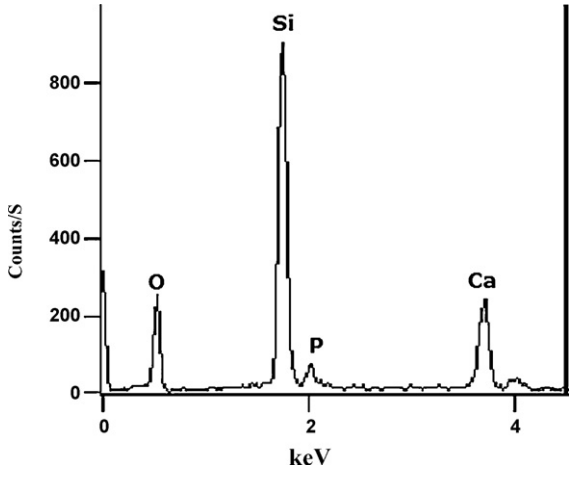

Fig. 1. Energy dispersive X-ray analysis (EDX) of the bioglass particles. The peaks of O, Si, P and Ca indicate the consisting elements of prepared bioglass.

Table 2
Bioactive glass estimated oxidic composition measured by X-ray fluorescence (XRF).

Oxide	Molar%
SiO_2	62.18
CaO	28.46
P_2O_5	9.25
LOI (loss on ignition)	0.11

3.1.2. EDXRF results for HA

The elementary composition results for the particles are listed in Table 3. As expected, the main elements detected calcium and phosphorus with an average Ca/P molar ratio of 1.93. As for minor components, silicon, magnesium and sodium were detected. Furthermore, traces of potassium, strontium, zinc, barium, vanadium, aluminum, manganese, lead, copper and iron were found. The results shown are the mean values of several examinations of particles by EDXRF. The Ca/P ratio of 1.93 is an approximate value as overlapping of different elements' peaks is possible, but this possibility was not investigated.

3.2. X-ray diffraction analysis

The XRD pattern of the prepared glass after heating at 600 °C for 2 h did not contain diffraction maxima, indicative of the internal disorder and the glassy nature of this material. The XRD pattern of the initial sample confirmed its amorphous nature, characterized by the broad diffraction bands (Fig. 2).

The X-ray diffraction spectrum showed that the HA particles prepared from bovine bone were highly crystalline (Fig. 3). The

Table 3
Elemental composition (mean value (standard deviation)) of the bone-derived HA particles measured by EDXRF.

Element	Concentration (% w/w)
Ca	41.77 (1.14)
P	16.71 (0.52)
Si	0.75 (0.18)
Mg	0.62 (0.20)
Na	0.40 (0.18)
K	0.24 (0.11)
Cl	0.12 (0.19)
Sr	0.11 (0.16)
S	0.083 (0. 10)
Zn	0.015 (0.02)
Ba	0.012 (0.01)
V	0.0045 (0.009)
Al	0.0020 (0.00052)
Mn	0.001 (0.00041)
Pb	0.0009 (0.001)
Cu	0.0005 (0.00036)
Fe	0.0001 (0.00024)

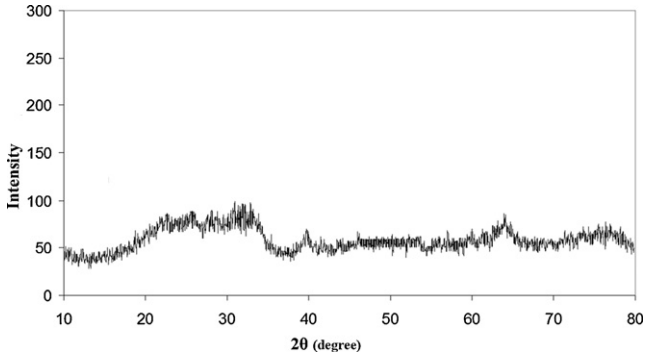

Fig. 2. XRD pattern of the prepared bioactive glass nanopowder. Intensity of diffraction vs. angle of radiation (2θ,°). No peak of diffraction could be observed.

HA spectra ($2\theta = 31.83°$) exactly conforms to natural HA XRD pattern that is reported in the literature [17]. Also only a minimal amount of MgO ($2\theta = 42.9°$) was detected in XRD pattern. This result is in agreement with previous reports [7,17]. There was no CaO detectable by XRD.

3.3. Scanning electron microscope

Fig. 4 shows SEM images of the bioactive glass particles. Heterogeneous surfaces consisting of random-sized particles with sharp edges can be seen.

Fig. 5(a) and (b) shows the microstructure of the prepared natural HA ceramic particles. The size of the hydroxyapatite crystals ranged from 50 to 500 nm. The HA crystal size in native bone, however, have been reported to be in 20–40 nm range [8]. Thus, the crystal size in the investigated ceramic was larger than that of natural bone.

3.4. Zeta potential

The zeta potential of these bioceramics, bioglass and bone-derived HA particles, was investigated in physiological saline. The zeta potential of the 63S bioactive glass particles ranged from -7.45 ± 0.74 mV at pH 5 to -16.18 ± 1.8 mV at a typical physiologic pH of 7.4. At pH 9 the zeta potential was -14.31 ± 1.4 mV. In summary, as shown in Fig. 6, the zeta potential varied with pH and was negative at acidic, neutral and basic pH values.

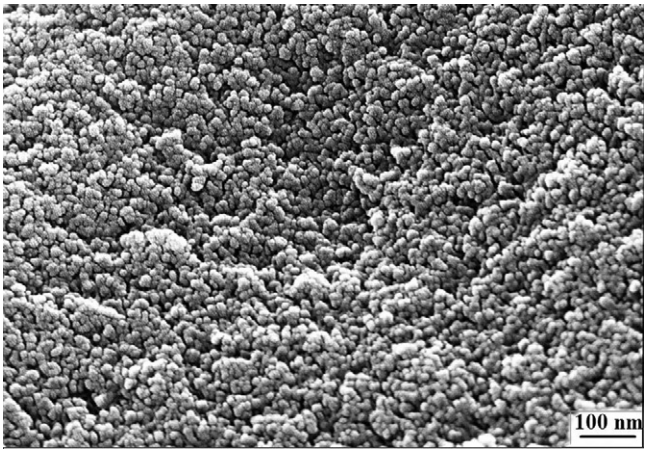

Fig. 4. SEM micrographs of the bioglass particles.

For HA, the zeta potential ranged from $+5.21 \pm 0.68$ mV at pH 3 to -16.40 ± 1.32 mV at pH 11. At pH 7.4 the zeta potential was -9.25 ± 0.9 mV. As shown in Fig. 7, the zeta potential varied with pH and was positive at acidic pH and negative at neutral and basic pH. At a typical physiologic pH of 7.4, the zeta potential was -9.25 ± 0.9 mV. The comparative results were presented in Table 4 for bioactive glass and natural HA.

3.5. The exothermal behavior

The total heat liberation and the rate of heat liberation of bioactive glass and bone-derived HA in different relative humidities and at 37 °C varied significantly (Figs. 8 and 9). Total heat liberation of bioglass in the relative humidity of more than 32% increased rapidly during the initial 15 h of hydration and then remained constant (Fig. 8a). The exothermal behavior of natural HA was almost similar to bioglass. The main difference was that the amount of liberated heat in HA hydration was several times less than

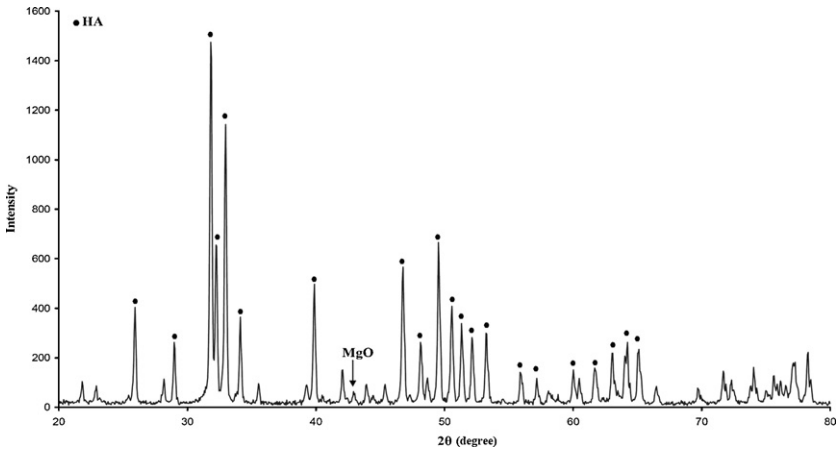

Fig. 3. X-ray diffraction spectrum of the HA particles.

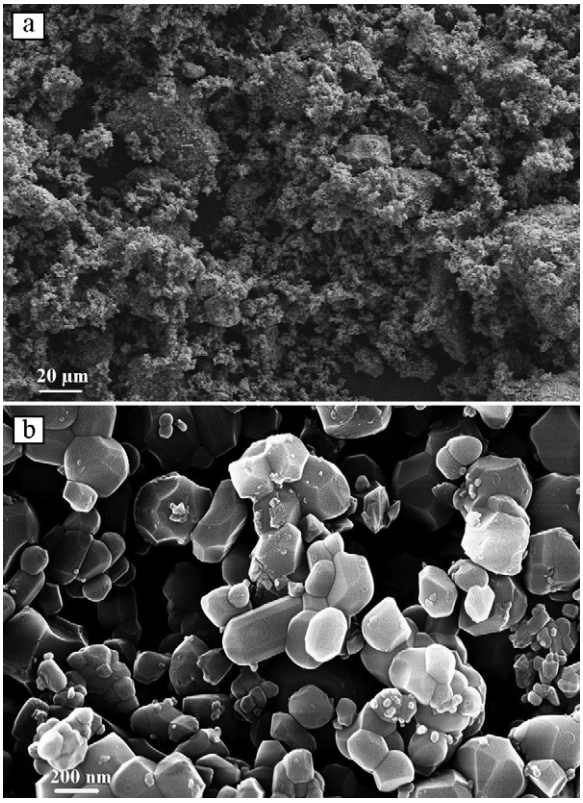

Fig. 5. SEM photographs of hydroxyapatite particles, showing the porous structure (a) and variety in crystal shape and size within the particles (b).

bioglass. In addition, after a quick increase in initial times, the liberated heat increased slowly up to 80 h (Fig. 8b).

The rate of heat liberation of bioactive glass and bone-derived HA is shown in Fig. 9. In 100% relative humidity the maximum of this rate was 4.6 mW/g. This value was almost 10 times more than the heat liberation rate of bone-derived HA (0.45 mW/g). In both kinds of these bioceramics, the rate of heat liberation increased rapidly at the early stage and then started to decrease.

4. Discussion

The EDX results (Fig. 1) indicated that the three main elements in bioactive glass particles (as expected) were Si, Ca and P. XRF analysis showed that the particles were composed of Si, Ca and P oxides. The molar percentages of these elements conformed approximately to the molar percentages of their oxides in prepared bioactive glass. These results showed that

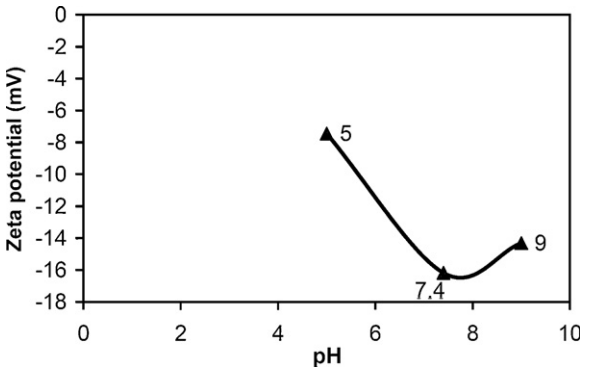

Fig. 6. Zeta potential at three different pH values for 63S bioglass particles in physiological saline at 37 °C.

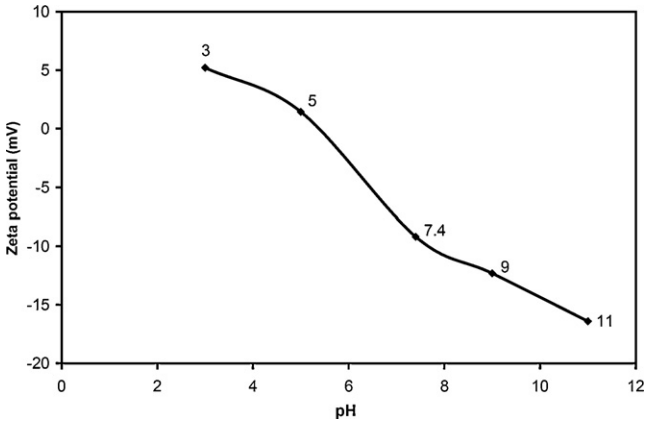

Fig. 7. Zeta potential at five different pH values for HA particles in physiological saline at 37 °C.

Table 4
Zeta potential for bioactive glass and bone-derived HA at different pH values.

Bioceramic material	Zeta potential (mV) at acidic pH	Zeta potential (mV) at neutral pH	Zeta potential (mV) at basic pH
Bioactive glass	−7.45	−16.18	−14.31
Bone-derived HA	+5.21	−9.25	−16.40

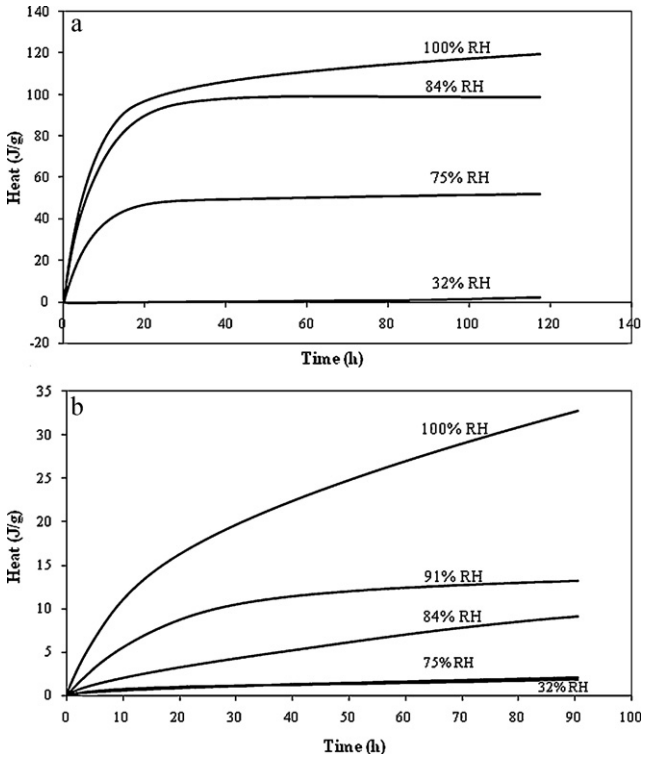

Fig. 8. Calorimetric curves showing the hydration heat of bioactive glass (a) and bone-derived HA (b) at 37 °C and different relative humidities.

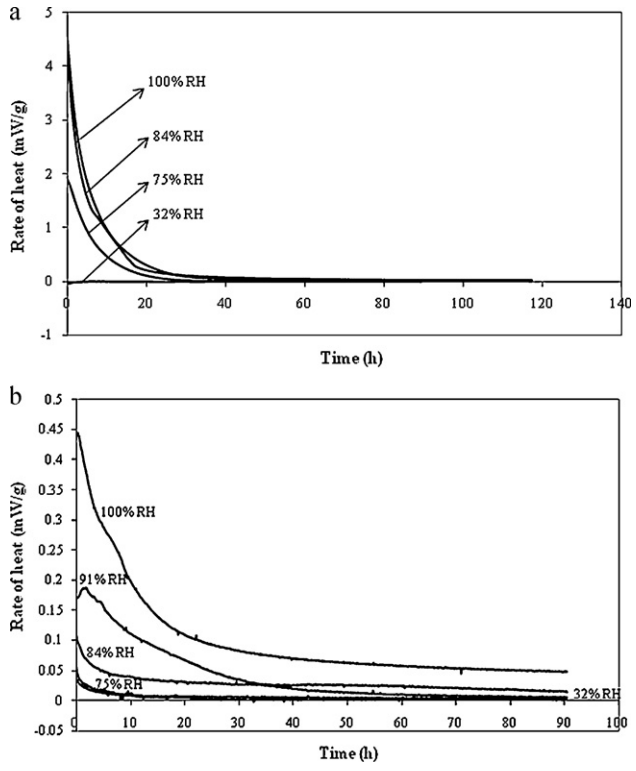

Fig. 9. Calorimetric curves showing the rate of heat liberation of bioactive glass (a) and bone-derived HA (b) at 37 °C and different relative humidities.

the composition of prepared bioglass was compatible with documented composition for sol–gel 63S bioactive glass [3]. The XRD pattern confirmed the amorphous nature of the particles, characterized by the broad diffraction bands. The result showed that there was no crystalline phase in bioglass particles, completely in agreement with previous reports [12,18]. Through XRD analysis, also it was confirmed that contrary to bioactive glass, prepared natural HA particles possessed a highly crystalline ceramic structure. EDXRF showed small amounts of trace elements in bone-derived HA including silicon, magnesium, sodium, potassium, strontium, zinc and barium (Table 3). This fact indicates the main difference between synthetic and natural HA. The existence of these elements in HA could be advantageous if this bioceramic is implanted in the human body and adjacent to the bone tissue. For example, Tian et al. have shown the positive influence of strontium on bone tissue in an in vivo experiment [19]. The role of trace elements in bone metabolism has been discussed in the literature [20].

According to SEM images (Fig. 4), the prepared bioactive glass particles were very fine and highly agglomerated as well [12,18]. These kinds of particles are expected to form through the sol–gel method. SEM images also showed that the crystal size of prepared HA was larger than HA crystals in natural bone. The much larger crystal size and the higher degree of fusion between individual crystals compared to the natural material are due to the manufacturing process. The degree of crystallite fusion and growth, however, varied among different ceramic particles and even within one particle (Fig. 5(b)).

The comparative results of zeta potential measurement of bioactive glass and HA have been presented in Table 4. The favorable effect of negative zeta potential on the attachment and proliferation of bone cells has been demonstrated [21,22]. We showed in this investigation that prepared 63S bioglass and bovine bone-derived HA particles produced by our methods have a natural negative zeta potential at pH 7.4 (found in many situations in vivo), in physiological saline (Table 4). This negative zeta potential for bioglass and bone-derived HA could be an advantageous property when these kinds of bioceramics are implanted in bone containing viable cells [21–23]. However, the zeta potential of 63S bioglass is approximately 2 times more than HA zeta potential at pH 7.4. In addition, contrary to bioglass, bone-derived HA demonstrated a positive zeta potential at acidic pH values. The difference between the measured zeta potential values for bioactive glass and bone-derived HA particles, could be related to different compounds and ions that exist in these bioceramics and their activities on the surface. This could be the subject of a future investigation.

According to the results obtained from calorimetry tests, it was observed that the amount and rate of the heat liberation from bioactive glass hydration process is considerably much more than that of the natural HA. The reason for this difference is related to the dissimilarity of their structure and the chemical composition. The biofunctionality of bioglass and HA is affected by these dissimilarities too [1,2,15]. Despite the fact that the maximum amount of heat libration rate in the bioglass hydration process is ten times higher than that of HA, it is lower when compared to bone cement and tricalcium silicate [24]. This fact is considered to be a priority for bioactive glass. Since the high heat generation during the hardening process can lead to local inflammation and thermal necrosis, it would be disadvantageous for injectable materials in use. Calcium phosphate cements (CPS) release a slight amount of heat during the hardening process and proved to be safe in use. The result of the exothermic experiment (Fig. 9) indicated that bioglass and natural HA released heat during the hydration process. The maximum rate of heat liberation (4.6 mW/g for bioglass) was lower as compared to CPC (8.4 mW/g) [24,25]. Certainly this little heat cannot be harmful for the adjacent soft and hard tissues in the human body.

5. Conclusion

63S bioactive glass and bovine bone-derived hydroxyapatite were produced. Amorphous structure of bioglass and completely crystalline structure of HA were indicated by XRD method. Chemical composition of 63S bioglass and natural HA were also determined and the results showed that in bone-derived HA, in addition to Ca and P, various trace elements were also present in slight amounts. This property could be the main difference between natural and synthetic bioceramic compositions.

The most important finding was a negative zeta potential for both 63S bioactive glass and natural HA in normal saline at a pH of 7.4. A negative zeta potential is thought to facilitate the bone cell activity, but some bioceramics such as synthetic HA particles do not have an intrinsically negative zeta potential. Having a

higher degree of zeta potential negativity especially in acidic pH values, bioglass has priority over HA. Finally, the exothermal behavior of natural HA and bioactive glass were compared. The results indicated that the amount of 63S bioglass heat liberation and its rate were about 10 times higher than that of bone-derived HA. This can be related to hydration mechanism and chemical composition of these materials. However, the amount of librated heat is in safe range and cannot be harmful for adjacent tissues.

References

[1] L.L. Hench, J.M. Polak, Third-generation biomedical materials, Science 163 (2002) 51–59.

[2] T.V. Thamaraiselvi, S. Rajeswari, Biological evaluation of bioceramic materials—a review, Trends Biomater. Artif. Organs 18 (2004) 9–17.

[3] L.L. Hench, The story of bioglass, J. Mater. Sci.: Mater. Med. 17 (2006) 967–973.

[4] L.D. Xynos, M.V.J. Hukkanen, J.J. Batten, L.D. Buttery, L.L. Hench, J.M. Polak, Bioglass t45S5 stimulates osteoblast turnover and enhances bone formation in vitro: implications and applications for bone tissue engineering, Calcif. Tissue Int. 67 (2000) 321–329.

[5] L.L. Hench, Genetic design of bioactive glass, J. Eur. Ceram. Soc. 29 (2009) 1257–1265.

[6] I.D. Xynos, A.J. Edgar, L.D. Buttery, L.L. Hench, J.M. Polak, Gene-expression profiling of human osteoblasts following treatment with the ionic products of bioglass 45S5 dissolution, J. Biomed. Mater. Res. 55 (2001) 151–157.

[7] C.V.M. Rodriguesa, et al., Characterization of a bovine collagen–hydroxyapatite composite scaffold for bone tissue engineering, Biomaterials 24 (2003) 4987–4997.

[8] A. Ruksudjarit, K. Pengpat, G. Rujijanagul, T. Tunkasiri, Synthesis and characterization of nanocrystalline hydroxyapatite from natural bovine bone, Curr. Appl. Phys. 8 (2007) 270–272.

[9] K.J.L. Burg, S. Porter, J.F. Kellam, Biomaterial developments for bone tissue engineering, Biomaterials 21 (2000) 2347–2359.

[10] K. Haberko, M.M. Bueko, J. Bgzezinska-Miecznik, M. Haberko, W. Mozgawa, T. Panz, A. Pyda, J. Zarebski, Natural hydroxyapatite—its behaviour during heat treatment, J. Eur. Ceram. Sci. 26 (2006) 537–542.

[11] R. Murugan, S. Ramakrishn, Bioresorbable composite bone paste using polysaccharide based nano hydroxyapatite, Biomaterials 25 (2004) 3829–3835.

[12] M.H. Fathi, A. Doostmohammadi, Preparation and characterization of sol–gel bioactive glass coating for improvement of biocompatibility of human body implant, Mater. Sci. Eng. A 474 (2008) 128–133.

[13] P. Sepulveda, J.R. Jones, L.L. Hench, Bioactive sol–gel foams for tissue repair, J. Biomed. Mater. Res. 59 (2002) 340–348.

[14] F.B. Bagambisa, U. Joos, W. Schilli, Mechanisms and structure of the bond between bone and hydroxyapatite, J. Biomed. Mater. Res. 27 (1993) 1047–1055.

[15] D.A. Oppermann, M.J. Crimp, D.M. Bement, In vitro stability predictions for the bone/hydroxyapatite composite system, J. Biomed. Mater. Res. 42 (1998) 412–416.

[16] A. Maria, Lactose and thermal analysis with special emphasis on microcalorimetry, Thermochim. Acta 248 (1995) 161–176.

[17] S. Joscheki, B. Nies, R. Krotz, Chemical and physicochemical characterization of porous hydroxyapatite ceramics made of natural bone, Biomaterials 21 (2000) 1645–1658.

[18] A. Balamurugan, G. Balossier, S. Kannan, J. Michel, A.H. Rebelo, J.M. Ferreira, Development and in vitro characterization of sol–gel derived $CaO–P_2O_5–SiO_2–ZnO$ bioglass, Acta Biomater. 3 (2007) 255–262.

[19] M. Tian, F. Cheng, W. Song, Y. Song, Y. Chen, C. Wan, X. Zhang, In vivo study of porous strontium-doped calcium polyphosphate scaffolds for bone substitute applications, J. Mater. Sci.: Mater. Med. 20 (2009) 1505–1512.

[20] B. Sandstrom, P. Walter, Role of trace elements for health promotion and disease prevention, Nutr. Res. 23 (1998) 1745.

[21] K. Cheng, W. Weng, H. Wang, S. Zhang, In vitro behavior of osteoblast-like cells on fluoridated hydroxyapatite coatings, Biomaterials 26 (2005) 6288–6295.

[22] R. Smeets, et al., A new biphasic osteoinductive calcium composite material with a negative zeta potential for bone augmentation, Head Face Med. 5 (2009) 13–20.

[23] N.C. Teng, S. Nakamura, Y. Takagi, Y. Yamashita, M. Ohgaki, K. Yamashita, A new approach to enhancement of bone formation by electrically polarized hydroxyapatite, J. Dent. Res. 80 (2001) 1925–1929.

[24] W. Zhao, J. Wang, W. Zhai, Z. Wang, J. Chang, The self-setting properties and in vitro bioactivity of tricalcium silicate, Biomaterials 26 (2005) 6113–6121.

[25] C.S. Liu, W. Gai, S.H. Pan, Z.S. Liu, The exothermal behavior in the hydration process of calcium phosphate cement, Biomaterials 24 (2003) 2995–3003.